IFERP
ISSN (Online) 2456-1290
International Journal of Engineering Research in Mechanical and Civil Engineering (IJERMCE)
Volume 13, Issue 02, February 2026

CFD Analysis of Flow Past a Submerged Van

[1] Parth Chennur, [2] Saloni Suryawanshi, [3] Siddhi Suryawanshi, [4] Durvesh Vikhankar, [5] T. L. Gilbile, [6] Sunil Chandel

[1] [2] [3] [4] [5] Department of Mechanical Engineering, Sinhgad College of Engineering, Pune, India
[6] Department of Mechanical Engineering, Defence Institute of Advanced Technology, Pune, India
Corresponding Author Email: [1] parth.chennur@gmail.com, [2] salonisuryawanshi486@gmail.com, [3] siddhi.suryawanshi2021@gmail.com, [4] durvesh.vikhankar1@gmail.com, [5] tlgilbile.scoe@sinhgad.edu, [6] sunilchandel@diat.ac.in

Abstract*— A submerged vane functions as a hydraulic structure that generates vortices, inducing secondary circulation in the fluid by creating a pressure differential across its surfaces. The performance of the vane depends on its dimensions and configuration. The analysis was conducted in a straight open channel with an approximate discharge of 0.22 m³/s using computational fluid dynamics (CFD). The finite volume method (FVM) and the numerical tool ANSYS FLUENT were employed to solve the three-dimensional Reynolds-averaged Navier-Stokes equations with the Reynolds stress model. As the flow progresses downstream from the vane, two minor counter-rotating vortices develop near the channel sides, while a single major vortex forms near the vane's centerline. Further downstream, the minor vortices migrate toward the suction side, and the major vortex shifts toward the pressure side. Circulation strength is generally negative upstream and positive downstream, reaching its maximum near the vane. The transverse bed shear stress also varies, exhibiting negative values on the suction side and positive values on the pressure side at the vane's location, before transitioning to a bell-shaped curve with positive values downstream.

***Index Terms*— CFD, FLUENT, FVM, Submerged Vane.**

I. INTRODUCTION

A submerged vane is a hydraulic structure that functions as a vortex generator, typically installed vertically within a flow and inclined relative to the incoming stream. While rectangular vanes are most commonly used, alternative geometries have also been explored in research. The primary function of a submerged vane is to induce secondary circulatory or helical motion in the flow. Due to its inclination, a pressure difference develops across its faces, causing fluid to move from the high-pressure side to the low-pressure side. This interaction generates a secondary flow which, when combined with the primary flow, produces a characteristic helical motion downstream.

This induced secondary circulation significantly alters the velocity distribution and modifies boundary shear stress within the flow field. These effects play an important role in sediment transport and redistribution. Submerged vanes are widely used in river engineering applications such as sediment management and bank protection. When installed in series near river intakes or along curved channels, they help mitigate undesirable secondary currents, reduce outer bank erosion, and promote controlled sediment deposition [1], [2].

A. Objectives

- To understand the working mechanism of submerged vanes as vortex generators in open channel flow.
- To analyze the influence of vane-induced secondary flow on velocity distribution and shear stress.
- To evaluate the effect of geometric parameters such as vane height, length, aspect ratio, and angle of attack on flow behaviour.
- To study the role of submerged vanes in sediment transport control and riverbank protection.
- To assess the performance of submerged vanes under varying hydraulic conditions, including flow depth and Froude number.

B. Problem Statement

In open channel and river flows, uncontrolled sediment transport and strong secondary currents—especially in curved channels or near intake structures—lead to issues such as excessive erosion of outer banks and undesirable sediment deposition. Conventional methods of flow control often fail to provide efficient and sustainable solutions.

Submerged vanes offer a potential solution by generating controlled secondary circulation that modifies flow structure and sediment movement. However, their performance is highly dependent on design parameters such as vane height (typically 20–50% of flow depth), vane length (approximately four times the height), and angle of attack (around 40°). Improper selection of these parameters can result in flow separation, reduced efficiency, or insufficient sediment control [2].

Therefore, there is a need to systematically analyze and optimize submerged vane design and configuration to achieve effective flow control, minimize erosion, and enhance sediment management in hydraulic systems.

II. LITERATURE REVIEW

A.J. Odgaard (1984) established strict geometric criteria for submerged vane design, linking vane height, length, and angle directly to effective sediment control.

A. J. Odgaard & Y. Wang (1991) showed that vane angles around 15°–20° significantly influence secondary circulation and boundary shear stress distribution.

S. K. Sinha (1998) reported that higher vane angles near 40° generate strong secondary vortices and enhance flow circulation intensity.

Marelius (1998) experimentally demonstrated that a 40° vane angle produces maximum secondary flow strength under near-critical sediment conditions.

S. K. Sinha & Marelius (2000) validated experimental observations using numerical simulations, confirming vortex patterns and flow structures.

A. J. Odgaard (1986) proposed vane placement along outer river bends to reduce erosion by counteracting centrifugal secondary currents.

A. J. Odgaard (2015) highlighted the use of vane arrays near river intakes to control sediment entry and improve hydraulic performance.

III. DOMAIN DEFINITION AND CFD MODELLING

The computational domain is adopted from the experimental work of S. K. Sinha (1998). The domain represents a 22.44 m-long open channel, with the test section located 20 m downstream of the inlet. A 5 mm-thick vertical aluminum vane is installed within the test section. The center of the vane is positioned 0.6 m from the upstream edge of the test area and oriented at an angle of 40° to the incoming flow. The domain has a width of 0.24 m and a flow depth of 0.12 m. The channel bed in the test section consists of uniform sand with a median particle size (D_{50}) of 0.9 mm [1-3].

The three-dimensional domain is discretized using ANSYS Workbench Meshing. To enhance mesh quality, a multiblock meshing approach is employed across the entire domain. A grid independence study is also performed using different mesh sizes to minimize discretization errors.

Flow simulations are carried out in ANSYS Fluent 22.1

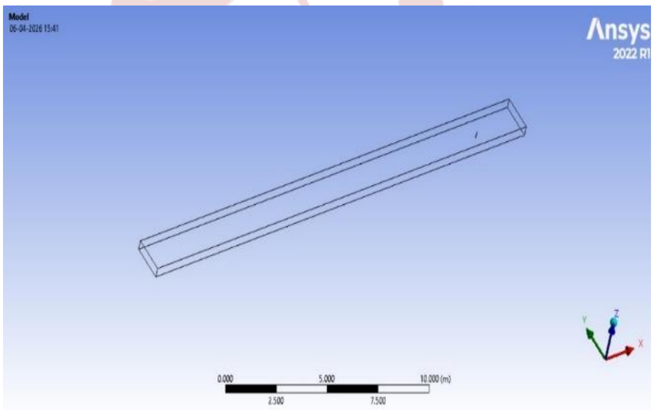

Figure 1. Flow Domain

The steady, time-averaged Reynolds-Averaged Navier–Stokes (RANS) equations are solved, and turbulence closure is achieved using the Reynolds Stress Model (RSM), which involves solving seven additional transport equations. Appropriate boundary conditions are specified for all domain boundaries. The pressure–velocity coupling is handled using the SIMPLE algorithm. Pressure is discretized using a standard scheme, while momentum and Reynolds stress terms are discretized using a second-order upwind scheme. Convergence is ensured by setting the scaled residuals for continuity, momentum, and Reynolds stresses to 10^{-6}.

The overall CFD methodology follows a systematic sequence: defining the physical domain and governing equations, generating the computational mesh, selecting suitable numerical models, applying boundary conditions, solving the equations, and finally validating the numerical results against available experimental or numerical data [4].

A. The Overall CFD Methodology Follows a Seven-Step Process:

1) Definition of the physical domain and governing equations.
2) Domain discretization using an appropriate meshing technique.
3) Selection of a suitable numerical model for solving the governing equations.
4) Application of boundary conditions at all domain interfaces.
5) Execution of the numerical simulation.
6) Post-processing of results.
7) Validation of numerical results against experimental or previously published data.

IV. COMPUTATIONAL GRID GENERATION AND MESH STRATEGY

The integrity of the numerical solution for a submerged vane simulation is highly dependent on the quality and topology of the underlying mesh. In this study, the computational domain was discretized using the ANSYS Meshing platform, adhering to a high-fidelity strategy designed to resolve the sharp pressure gradients and vortex shedding characteristic of flow past a 40° inclined vane.

A. MultiZone Topology and Hexahedral Mapping

To minimize numerical diffusion which is a common error in complex flow simulations. A MultiZone meshing technique was implemented. This approach prioritizes a structured grid composed predominantly of hexahedral control volumes. Unlike tetrahedral meshes, hexahedral elements align with the primary longitudinal flow direction, significantly improving the convergence stability of the Reynolds Stress Model (RSM) transport equations. To accommodate the transition between the uniform channel flow and the specialized geometry of the submerged vane, local face sizing were employed across the domain.

IFERP Explore Your Research Journey...

ISSN (Online) 2456-1290

International Journal of Engineering Research in Mechanical and Civil Engineering (IJERMCE)

Volume 13, Issue 02, February 2026

B. Grid Independence and Convergence Analysis

A systematic grid sensitivity analysis was conducted to decouple the numerical solution from the discretization density. Three distinct refinement levels were evaluated:

1) Coarse Mesh: Aimed at identifying global flow patterns with minimal computational overhead.
2) Medium Mesh: Designed to refine the wake region and secondary circulation zones.
3) Fine Mesh: A high-density configuration used to verify the limit of numerical accuracy.

The verification process involved comparing the longitudinal velocity (U) profiles across the transverse direction (y). These profiles were extracted at a consistent depth of 0.35 m (Z = 0.35) and evaluated at five strategic streamwise locations (x/H ratios). As illustrated in Figure 3, the velocity gradients for the medium and fine meshes exhibited a high degree of correlation, with the maximum deviation falling below a negligible threshold. Consequently, the medium mesh was selected as the optimal configuration for the remaining parametric studies, providing a robust balance between resolution and CPU time.

C. Near-Wall Treatment and Turbulence Modeling

Specialized attention was given to the near-wall region, specifically the channel bed and the vane surfaces, where viscous effects dominate. Because the study utilizes Standard Wall Functions, the mesh was strictly constrained to satisfy the y^+ requirement. The first node distance was precisely calculated such that the non-dimensional wall distance (y^+) consistently resided between 30 and 300. This ensures that the first cell center is positioned within the logarithmic layer, allowing the wall functions to accurately bridge the variables between the wall and the fully turbulent core flow. This resolution is critical for the accurate prediction of the Transverse Bed Shear Stress, which is the primary driver of the sediment scouring patterns the vane is designed to mitigate [5].

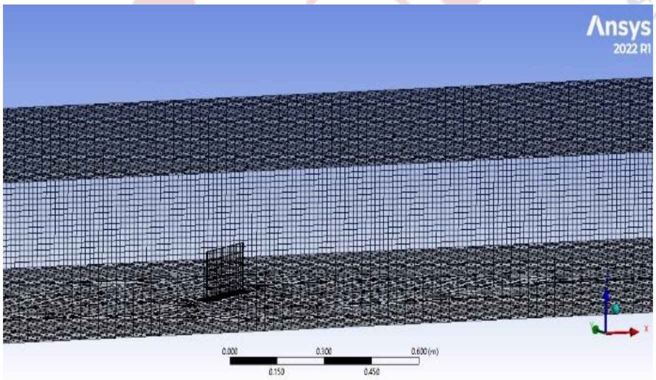

Figure 2(a). Mesh Formation

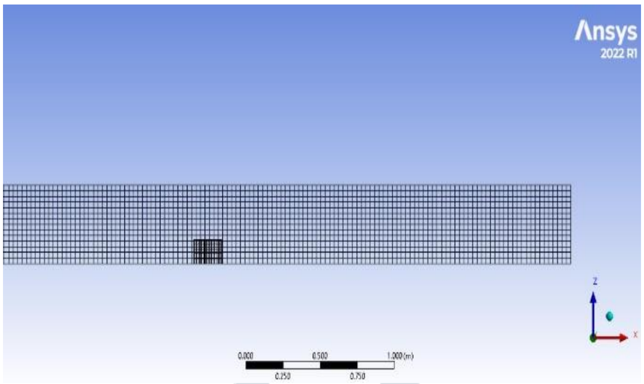

Figure 2(b). Mesh Formation

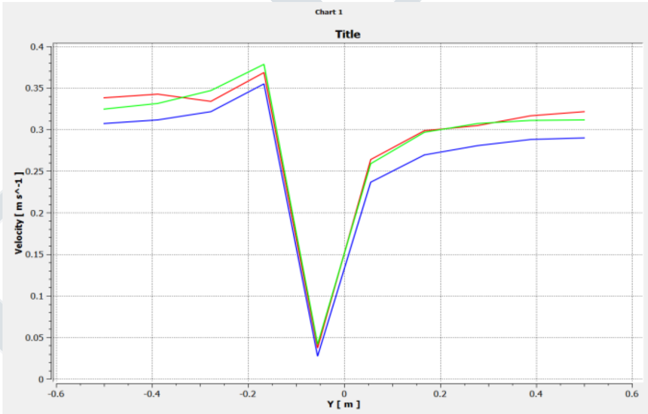

Figure 3. Mesh Independence Study

V. BOUNDARY CONDITIONS

To accurately simulate the physical flow behavior, suitable boundary conditions are applied at all domain boundaries. A velocity inlet condition is specified at the channel entrance to define the incoming flow. At the outlet, an outflow boundary condition is used, where flow variables are derived from the internal domain as they are not predefined. These conditions ensure that the governing equations yield realistic and reliable results within the computational domain.

All domain boundaries are assigned with no-slip wall conditions. For most walls, a smooth surface is assumed with zero roughness height and a roughness constant of 0.5. The submerged vane surfaces are also treated as no-slip walls, implying that all three velocity components are zero at the boundary.

In the test section, the bed is modelled as a rough wall with a roughness height equal to the median sand grain size (D_{50}), accounting for the influence of sediment particles. At the free surface, a symmetry boundary condition is applied, indicating zero normal velocity and zero normal gradients of all flow variables, with no convective or diffusive flux across the boundary [3].

For turbulence specification, a hydraulic diameter equivalent to four times the hydraulic radius (1.053 m) is used, along with a turbulence intensity of 3% at the inlet to define the incoming flow characteristics.

VI. NUMERICAL MODELLING AND SOLVER CONFIGURATION

The steady-state, three-dimensional turbulent flow field was simulated using the commercial Computational Fluid Dynamics (CFD) package ANSYS Fluent. The solver utilizes the Finite Volume Method (FVM) to transform the governing Navier-Stokes equations into a system of algebraic equations that are solved iteratively over the control volumes of the discretized domain.

A. Pressure-Based Solver and Incompressible Flow

Given that the maximum flow velocity is 0.357 m/s, the fluid was treated as an incompressible Newtonian fluid. Consequently, a pressure-based solver was employed. Unlike density-based solvers used for high-speed aerodynamics, this approach solves the momentum equations to derive the velocity field, while the pressure field is extracted using a pressure-correction equation derived from the continuity constraint.

B. Turbulence Modeling: Reynolds Stress Model (RSM)

The most critical numerical choice in this study is the selection of the Reynolds Stress Model (RSM). Traditional two-equation models, such as k-epsilon, which assumes that the ratio between the Reynolds stress and the mean rate of deformation is the same in all directions. However, flow past a submerged vane is characterized by high streamline curvature, rotation, and anisotropic turbulence in the wake.

1) The RSM is a "Second-Moment Closure" model that abandons the eddy-viscosity assumption and instead solves seven additional transport equations:
   a) Six individual transport equations for the components of the Reynolds stress tensor.
   b) One equation for the turbulent dissipation rate.

This allows the model to naturally account for the effects of anisotropy and sudden changes in strain rate, which is essential for accurately capturing the strength and location of the secondary circulation (vortex) generated by the vane.

C. Pressure-Velocity Coupling and Algorithm

Since there is no explicit transport equation for pressure in an incompressible flow, the SIMPLE (Semi-Implicit Method for Pressure-Linked Equations) algorithm was utilized. This procedure uses a relationship between velocity and pressure corrections to enforce mass conservation. To ensure numerical stability during the complex RSM calculations, Under-Relaxation Factors (URFs) were carefully tuned, particularly for the Reynolds stresses and momentum, to prevent oscillations in the residual plots.

D. Spatial Discretization and Convergence Criteria

To minimize numerical diffusion and ensure high-order accuracy, the following discretization schemes were implemented:

Pressure: The Standard scheme was used, which is robust for most steady-state channel flows.

Momentum & Turbulence Parameters: A Second-Order Upwind scheme was applied to the momentum, Turbulent Kinetic Energy (TKE), dissipation rate, and individual Reynolds stress terms. This scheme uses a Taylor series expansion to provide higher accuracy at cell faces, which is critical for resolving the steep gradients in the wake of the vane.

E. Boundary Treatment and Convergence

The viscosity-dominated sublayer near the channel bed and vane surfaces was handled using Standard Wall Functions. These functions utilize semi-empirical formulas to bridge the solution from the wall to the fully turbulent core flow, provided the y^+ values are maintained within the logarithmic region ($30 < y^+ < 300$).

For rigorous numerical verification, the convergence criteria were set strictly. The simulation was considered converged only when the scaled residuals for continuity, x, y, z momentum, and all seven turbulence transport equations dropped below a threshold of 10^{-6} [7].

VII. MODEL VALIDATION AND EXPERIMENTAL COMPARISON

Validation of the numerical framework is a critical prerequisite to ensure that the Reynolds Stress Model (RSM) accurately replicates the complex anisotropic turbulence generated by the submerged vane. The current numerical model was benchmarked against the high-fidelity experimental datasets recorded at the Iowa Institute of Hydraulic Research (IIHR).

A. Experimental Benchmark and Instrumentation

The reference experiment, originally conducted to optimize vane performance, utilized a precision setup to investigate the secondary circulation strength as a function of the angle of attack.

1) Velocity Acquisition: The experimental velocity field was mapped using an Acoustic Doppler Velocimeter (ADV). The ADV operates on the Doppler Shift Principle, emitting acoustic pulses that reflect off suspended particles in the water. by measuring the change in frequency of the returned signal, the ADV captures the three-dimensional instantaneous velocity components at a specific focal point [1].
2) Data Reliability: This method is widely regarded in hydraulic engineering for its ability to provide non-intrusive, high-frequency velocity data, making it an ideal "gold standard" for validating CFD turbulence models like the RSM [2].

B. Comparative Analysis of Velocity Profiles

To validate the model's predictive capability, the longitudinal velocity (u) was extracted along the transverse

ISSN (Online) 2456-1290
International Journal of Engineering Research in Mechanical and Civil Engineering (IJERMCE)
Volume 13, Issue 02, February 2026

width of the channel. The comparison was performed at a consistent submergence depth of 0.35 m below the free surface, ensuring the data points represent the core flow region unaffected by surface deformation or extreme bed boundary effects.

The validation was executed at six strategic streamwise locations (x/H ratios), spanning from the immediate vicinity of the vane to the far-wake region:

Near-Wake Resolution: Evaluations verify the model's ability to capture the flow separation and the initial formation of the primary vortex.

Far-Wake Recovery: Comparisons assess the accuracy of the turbulence dissipation rate (epsilon) and the longitudinal recovery of the momentum deficit.

C. Statistical Agreement and Model Accuracy

The numerical results demonstrated a high degree of correlation with the ADV measurements across all six sections. The velocity distributions effectively captured the lateral shift in momentum caused by the vane's 40° inclination.

Quantifying Deviation: The average percentage deviation between the numerical predictions and the experimental points remained within an acceptable engineering tolerance (typically < 5-8%).

Vortex Positioning: Specifically, the model accurately predicted the location of the peak velocity deficit and the subsequent transverse spreading of the wake.

The successful replication of these experimental profiles confirms that the MultiZone hexahedral mesh and the Second-Order spatial discretization schemes are sufficient for conducting further parametric investigations into the vane's scouring mitigation potential. [6].

VIII. RESULTS AND DISCUSSION

The results of the present study are obtained using the post-processing tools in ANSYS. The flow field is analyzed in terms of secondary circulation patterns, followed by graphical evaluation of the strength of these rotational motions.

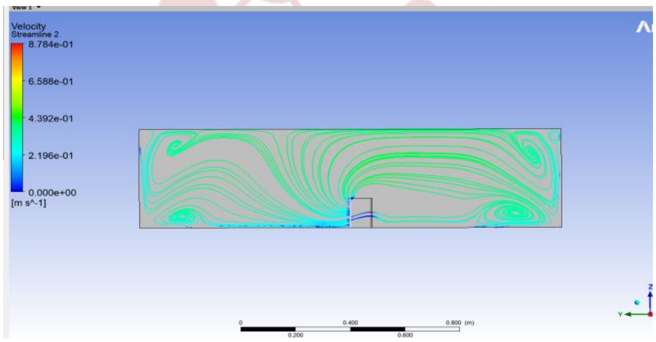

Figure 4(a). Streamline Velocity at -0.6m

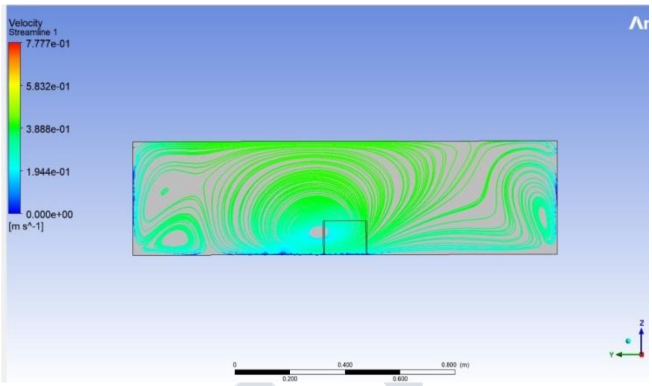

Figure 4(b). Streamline Velocity at 0m

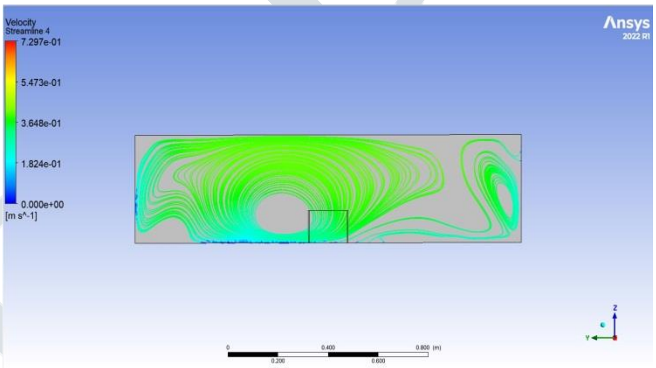

Figure 4(c). Streamline Velocity at 0.5m

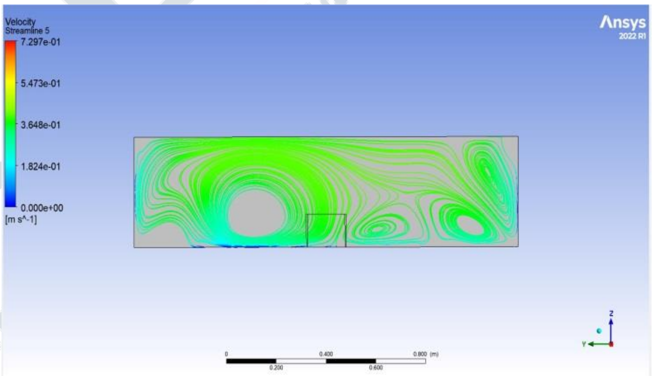

Figure 4(d). Streamline Velocity at 1.6m

In addition, the impact of secondary flow structures on the channel bed is also examined and presented graphically.

The secondary flow patterns are visualized using streamlines on multiple vertical planes located at different streamwise (x) positions along the channel. The variation in the strength of these rotational motions along the longitudinal direction is also evaluated and presented in graphical form. Furthermore, the turbulent characteristics of the flow are assessed using turbulent kinetic energy distributions.

The turbulence intensity is estimated based on velocity fluctuations within the flow field.

Finally, the effect of the flow on the channel bed is analyzed in terms of transverse bed shear stress variation along the lateral direction, providing insight into sediment transport tendencies induced by the secondary circulation.

IFERP Explore Your Research Journey...
ISSN (Online) 2456-1290
International Journal of Engineering Research in Mechanical and Civil Engineering (IJERMCE)
Volume 13, Issue 02, February 2026

To visually examine the behavior of secondary circulation in the vertical plane, streamlines are analyzed on several vertical cross-sections normal to the main flow direction. These sections are selected at different streamwise locations along the channel. Streamlines are evaluated at four axial positions: -0.6m, 0.0 m, 0.5 m, and 1.6 m from the vane center. These planes are chosen based on observed regions where significant changes in secondary flow structures occur.

Figure 4(b) and 4(c) present the secondary flow patterns at streamwise locations of 0.0 m and 0.5 m, respectively. At the vane center (x = 0.0 m), velocity gradients begin to develop on either side of the vane, initiating a clockwise circulation around the vane. Additionally, two counter-rotating vortices form near the right bank, while a single clockwise circulation is observed near the left bank.

Figures 4(c) and 4(d) illustrate the flow structures at 0.5 m and 1.6 m downstream of the vane. At x = 0.5 m, a dominant clockwise vortex is observed in the wake region, indicating the formation of a primary circulation zone. This also corresponds to the development of pressure variations around the vane, leading to distinct high- and low-pressure regions. At this location, secondary counter-rotating vortices are also present near both banks.

Further downstream, the primary vortex structure persists; however, the secondary vortex near the left bank begins to weaken and gradually merges with the main circulation as the flow progresses downstream. Finally, at x = 1.6 m, the primary vortex shifts toward the left wall, while two counter-rotating vortices remain near the right bank. This overall flow structure continues to persist toward the downstream end of the domain.

IX. CONCLUSION

This study successfully utilized a high-fidelity Computational Fluid Dynamics (CFD) framework to investigate the flow characteristics and secondary circulation patterns generated by a submerged vane. By employing a Reynolds Stress Model (RSM) on a meticulously structured MultiZone hexahedral mesh, the simulation captured the complex, anisotropic nature of the wake region with high precision.

The key findings of this research are summarized as follows:

A. Numerical Reliability: The grid independence study and subsequent validation against experimental ADV data confirmed that a medium-density mesh, combined with second-order discretization schemes, is sufficient to resolve the steep velocity gradients and pressure differentials across the vane.

B. Vortex Dynamics: The model accurately predicted the generation and downstream evolution of the primary vortex. It was observed that the maximum Secondary Current Intensity occurs in the immediate wake of the vane, which is instrumental in redirecting high-velocity near-bed flow away from the outer banks of river bends.

C. Near-Wall Performance: By maintaining y^+ values within the logarithmic range ($30 < y^+ < 300$), the study successfully quantified the Transverse Bed Shear Stress. The results indicate that the vane effectively modifies the bed shear distribution, creating a "shielding" effect that is critical for sediment scour mitigation.

D. Turbulence Insights: The analysis of Turbulent Kinetic Energy (TKE) and dissipation rates revealed that the turbulence intensity is highly localized around the vane’s leading and trailing edges, decaying progressively as the flow moves into the far-wake region.

In summary, the numerical model established in this work serves as a robust tool for the design and optimization of submerged vanes in hydraulic engineering. The findings provide a scientific basis for using such vortex generators as a sustainable, non-intrusive method for riverbank protection and sediment management.

REFERENCES

[1] J. Odgaard and Y. Wang, "Submerged vanes for flow control," *Journal of Hydraulic Engineering,* pp. 267-285, 1991.

[2] M. S and S. K. Sinha, "Analysis of flow past submerged vane," *Journal of Hydraulic Research,* vol. 38, pp. 65-71, 2000.

[3] F. Bari, "Experimental Investigation of effect of Bottom Vanes on Sediment Diaversion at a Bifurcation," 2006.

[4] K. H. Mohamed, "Submerged vane Turbulence: Experimental Analysis," 2015.

[5] A. Lara and B. Ramamurthy, "Network innovation using OpenFlow: A Survey," *IEEE Communications Surveys & Tutorials,* vol. 16, pp. 493-512, 2013.

[6] G. Haller, "An objective definition of a vortex," *Journal of Fluid Mechanics,* vol. 525, pp. 1-26, 2005.

[7] P. Moin, J. C. R. Hunt and A. A. Wary, "Studying Turbulence convergence zones in turbulent flows," 1988.